Vacancy-Mediated and Exchange Diffusion in a Pb/Cu(111) Surface Alloy: Concurrent Diffusion on Two Length Scales

M. L. Anderson, M. J. D'Amato, P. J. Feibelman, and B. S. Swartzentruber
Sandia National Laboratories, Albuquerque, New Mexico 87185
(Received 10 September 2002; published 24 March 2003)

Pb diffuses in a Pb/Cu(111) surface alloy predominantly by exchange with surface vacancies and, much less frequently, by exchange with thermal Cu adatoms. Because the infrequent adatom exchanges transport Pb atoms much farther, both processes affect observations of Pb transport in the Pb/Cu(111) surface alloy.

DOI: 10.1103/PhysRevLett.90.126102 PACS numbers: 68.35.Fx, 05.40.Fb, 07.79.Cz, 66.30.Jt

A common thread in recent studies of kinetics on metal crystal surfaces is whether mass transport occurs predominantly via adatom or vacancy-mediated processes [1–3], and, if adatoms are involved, whether diffusion occurs by simple hopping or exchange processes [4]. The formation and migration energies of the diffusing species are the key factors. On close-packed fcc(111) surfaces [5], where vacancy and adatom formation energies are comparable, the vacancy migration barrier is substantially higher. Thus, vacancy-mediated diffusion is unexpected. Likewise, high coordination makes exchange costly. Therefore, mobile adatom attachment and detachment at steps should dominate the equilibration process.

Many kinetic processes may occur in the decay of metastable structures, or in self-assembly, but their relative rates can differ by orders of magnitude because of exponential dependence on activation energy. However, the frequent processes may not dominate decay kinetics. They may be ineffective at mass transport and thus contribute only to fluctuations. For example, in the coarsening of monolayer-high islands on metal surfaces or the decay of multilayer stacks of islands [6,7], processes that transport mass between islands contribute. Transport around the edges of the islands contributes only to fluctuations about the metastable configuration.

Recently, Plass *et al.* discovered that a rich variety of nanostructures self-assembles in Pb deposition on the Cu(111) surface [8], changing as a function of surface coverage of Pb. That the equilibrium patterns form as they do testifies to very rapid mass transport kinetics between the two phases; however, the specific mechanisms are unknown.

In this Letter, we investigate the mass transport kinetics of the Pb/Cu(111) surface alloy in the dilute limit. We measure the diffusion of Pb atoms on two length scales using scanning tunneling microscopy (STM), and calculate the relevant energetics using first-principles electronic total-energy calculations. The short-distance motion of individual atoms is extracted from comparison of consecutive STM images. Long displacements are determined from the decay of an initially nonuniform concentration profile. Both measurements are crucial in determining the physical processes.

The experiments are performed in ultrahigh vacuum (base pressure 1×10^{-10} torr) using a variable-temperature STM. The Cu surface is cleaned by repeated cycles of 25 min sputtering with 1 keV Ne^+ ions followed by 10 min annealing at ~600 °C. Pb atoms are evaporated from bulk Pb in a resistively heated tungsten wire basket. The deposition rate is about 1 monolayer(ML)/min. STM images are acquired in constant current mode (~ 50 pA) with a tungsten tip at sample biases between −0.050 and −1 V. It is very difficult to image the atoms of the bulk truncated Cu(111) surface, but the embedded Pb atoms are seen quite readily as slight protrusions in the surface.

To test our interpretation of the measurements, we calculated configuration energies from first principles using the VASP [9] electronic total-energy code, its ultrasoft pseudopotentials [10], and the Perdew-Wang 1991 version of the generalized gradient approximation [11]. The computational unit cells were $4 \times 3\sqrt{3} \times 4$ layers. The surface Brillouin zone was sampled with 16 k points. To compute transition barrier energies, we used the Jónsson-Mills-Jacobsen nudged elastic band method [12].

Although Pb is immiscible in bulk Cu, at low coverage it is energetically favorable for a Pb to replace a Cu atom in the outermost layer of the crystal, forming a surface alloy [13]. The thermodynamically stable phase has embedded Pb atoms uniformly distributed throughout the surface layer.

The kinetic pathway from deposition to equilibrium is somewhat tortuous. The calculated energy difference between an adsorbed Pb atom and an embedded Pb atom surrounded by Cu is 0.38 eV. This means there is a strong driving force to embed in the outer layer. Although the Pb atoms are deposited randomly on the surface, the barrier to embed directly in the middle of a terrace is high (calculated 1.17 eV). On the other hand, the surface diffusion barrier for Pb adatoms is very small (~ 0.03 eV). At 400 K, the relative rates for these two processes is on the order of 10^{15}. Thus, a diffusing Pb adatom can visit virtually the entire sample before incorporating in the middle of a terrace via the exchange mechanism. In

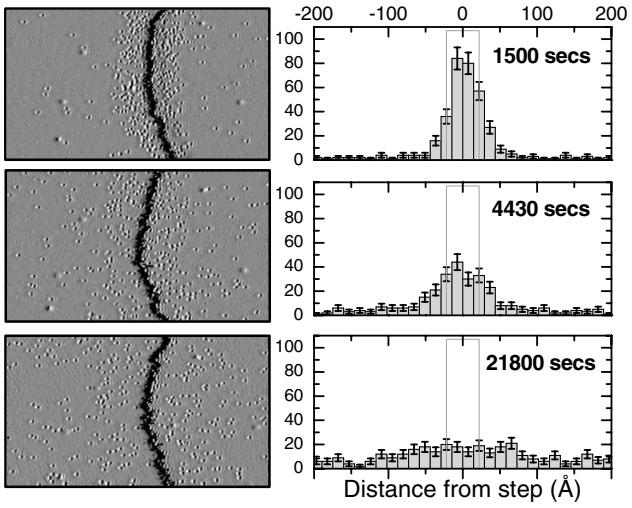

FIG. 1. Derivative-mode STM images showing the evolution of the embedded Pb concentration profile as a function of time. The upper terrace is on the left. Scale: 550×366 Å^2. Histograms show the atom concentration versus distance from step. The light gray line shows the initial concentration profile used in the predictive models.

practice, the Pb adatoms quickly find a step and incorporate there, leading to an initial metastable configuration of Pb-decorated steps immediately after deposition. We find that the initial concentration profile is a stripe of surface alloy with ~0.2 ML of Pb whose width depends on the amount of deposited Pb and the widths of neighboring terraces. For the conditions shown in Fig. 1, the width of the initial alloy stripe is about 25 Å.

Approach to equilibrium then proceeds through slow spreading of the nonuniform concentration distribution as the embedded Pb atoms diffuse in the surface layer. The three images displayed in Fig. 1 were taken from an STM movie near the beginning, middle, and end of a six-hour series, acquired at 400 K.

We quantify the Pb concentration profile versus time by marking the location of every Pb atom in each image, binning the atoms according to the shortest distance to the step, which adjusts for the slight curvature of the step along the y direction in the data. Concentration profiles are plotted beside their respective images in Fig. 1. We digitized 12 profiles at equally spaced time intervals throughout this six-hour data set.

The solution of the one-dimensional diffusion equation for the concentration using the initial boundary condition of a stripe of width, W, is

$$c(x,t) = \frac{A}{2}\left\{\mathrm{erf}\left(\frac{x+\frac{W}{2}}{\sqrt{4Dt}}\right) - \mathrm{erf}\left(\frac{x-\frac{W}{2}}{\sqrt{4Dt}}\right)\right\}.$$

Here, A is the amplitude of the distribution, determined by the initial number of deposited Pb atoms incorporated at the step, and D is the diffusion coefficient. The diffusion coefficient is extracted from measurements of the

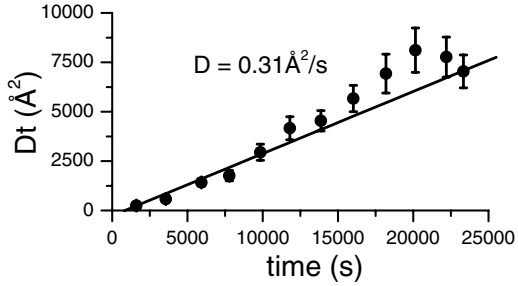

FIG. 2. Width of the concentration profile versus time, from which the diffusivity is extracted.

width of the distribution (i.e., Dt) versus time (Fig. 2). The diffusivity describing the profile decay is 0.31 Å^2/s.

For comparison, we also measure the diffusion statistics of individual Pb atoms explicitly from STM movies in which all of the atoms are marked. Figure 3 shows two consecutive frames, separated by 14 s, from an STM movie taken at 400 K. Several of the Pb atoms diffused in the time interval between frames. For an isotropic surface, $\langle x^2 \rangle = \langle y^2 \rangle = 2Dt$. Analyzing the measured mean square displacement of individual atoms in the data set of Fig. 1 yields $D = 0.032$ Å^2/s, *which is an order of magnitude smaller than that extracted from the profile decay.* This surprise means the atom-scale diffusivity is *much* too slow to account for the evolution of the

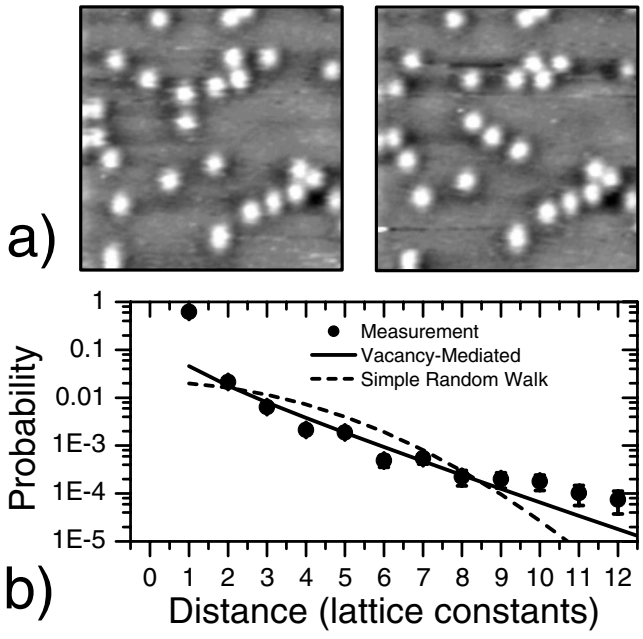

FIG. 3. (a) Two consecutive frames (separated by 14 s) from a 100×100 Å^2 STM movie acquired at 400 K. The embedded Pb atoms are seen as white protrusions. (b) Measured diffusion length distribution (solid circles). The solid line is the expected distribution for vacancy-mediated diffusion, and the dotted line is the expected Gaussian distribution from a simple random walk process.

concentration profile [14]. Clearly, the basic diffusion picture is too simple to describe the underlying physics completely.

To test whether Pb-Pb interactions are responsible for the unexpectedly rapid spreading of the concentration profile, we measured the dependence of the diffusivity on Pb concentration. We compared regions near to and far from the steps at early and late times and found no systematic difference at the dilute concentrations studied in this work. Therefore, Pb-Pb interactions do not affect the spreading of the concentration profile.

To learn the cause of the discrepancy, we need to determine how the embedded Pb atoms move, and therefore must analyze the diffusion statistics in more detail. Following van Gastel [15], we extract a displacement distribution by measuring the difference in position of atoms in sequential frames [Fig. 3(b)]. This distribution is the probability that an atom has moved a certain distance in a fixed time interval, and can be a signature of the diffusion process.

For Pb/Cu(111), the important information is in the slowly decaying tail, which drops much more slowly than a Gaussian. The slow decay implies that there are more multiple-lattice-constant diffusion lengths on a short time scale than expected in a simple random walk. This is a signature of vacancy assisted diffusion [16]. Like embedded Pd [3] and In [2] in the outer layer of Cu(001), diffusion of embedded Pb in Cu(111) occurs via exchange with surface vacancies. In the vacancy-mediated process, diffusion proceeds through repeated exchanges of a Pb atom with a surface vacancy leading to correlations on a short time scale [17]. When a vacancy is in the immediate neighborhood of a Pb atom, its likelihood is high of exchanging with the Pb atom several times in rapid succession. In contrast, a Pb atom is immobile when there are no vacancies nearby. Thus, short correlated bursts of rapid motion are separated by longer uncorrelated time intervals [18]. The time scale of each burst cannot be resolved by STM—only the time between bursts can [3]. We adopt the view that a diffusion event is comprised of a single burst. The rate at which vacancy-mediated diffusion occurs depends on the population of thermal vacancies and their migration. These quantities are determined by the vacancy formation energy and the vacancy migration barrier, which are calculated to be 0.76 and 0.68 eV, respectively. We extract the average diffusion event rate from the STM movies by counting how many Pb atoms change position between frames [19]. From the data acquired at 400 K at an image rate of 14 s/frame, we measure a diffusion event probability of 0.056/frame, which yields a diffusion event rate, $r = 0.0041/\mathrm{s}$. Assuming an attempt frequency between 10^{12} and 10^{13} Hz (and a factor of 6 in directional degeneracy corresponding to hexagonal symmetry) yields an effective activation barrier for diffusion of 1.24 ± 0.04 eV, a bit lower than the calculated sum of the vacancy formation and migration energies (1.44 eV). We extract the average length of the diffusion events from the measured mean square displacement and diffusion event rate, and find it to be 1.4 lattice constants. A diffusion event length greater than a lattice constant is another result of vacancy-mediated diffusion [20], arising strictly from the diffusion statistics of a vacancy that lead to bursts of single events. This is in contrast to some systems in which true long jumps are observed [19,21].

The solution to our problem comes from closer inspection of the atom-diffusion data. In addition to the vacancy-mediated diffusion events described above, we find another type of event that occurs *much* less frequently. Specifically, we see Pb atoms occasionally appear or disappear in the image. These events are completely uncorrelated with each other temporally or spatially, and occur roughly 40–80 times less often than the vacancy-mediated diffusion events. In the data shown in Fig. 1, a sudden-appearance event occurs with probability $5 \times 10^{-5}/\mathrm{s/Pb}$ atom (average time 5.5 h). Because they are rare, these events contribute insignificantly to the statistics of local vacancy-mediated diffusion. *However, they cannot be dismissed in analyzing the concentration-profile decay.*

To include the effect of appearance and disappearance events on the profile decay, we add two terms to the equation for mass transport. The first, describing disappearance of embedded Pb atoms from the surface layer, is proportional to the local concentration of embedded Pb atoms. The second describes the sudden appearance of embedded Pb atoms in the surface layer. For low coverage, it is independent of concentration. By detailed balance, the two total rates must be equal. Thus, the modified diffusion equation becomes

$$\frac{dc(x,t)}{dt} = D\frac{d^2c(x,t)}{dx^2} - rc(x,t) + r\langle c\rangle,$$

where $\langle c\rangle$ is the average concentration of embedded Pb atoms. For the initial boundary condition of a finite width stripe, its solution is

$$c(x,t) = \frac{A}{2}e^{-rt}\left\{\mathrm{erf}\left(\frac{x+\frac{W}{2}}{\sqrt{4Dt}}\right) - \mathrm{erf}\left(\frac{x-\frac{W}{2}}{\sqrt{4Dt}}\right)\right\} + \langle c\rangle(1-e^{-rt}),$$

a predictive equation for the time evolution of the concentration profile, in which all of the parameters are measured. $D = 0.032\ \mathrm{\AA}^2/\mathrm{s}$ is the vacancy-mediated diffusivity and $r = 5 \times 10^{-5}/\mathrm{s/Pb}$ atom is the rate of sudden appearance and disappearance events. To see how well this equation describes reality, we start from the initial profile and evolve the concentration to find when the predicted profiles match the measured ones (Fig. 4). That predicted time versus real time is linear, with a slope close to unity, means that the time evolution is accurately described throughout the decay. Thus, all of the essential processes are included.

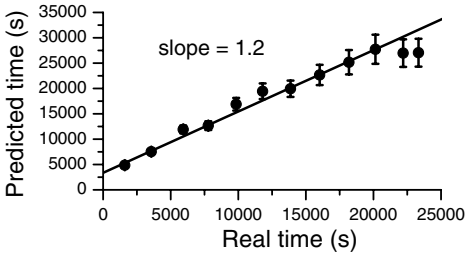

FIG. 4. Predicted evolution of the concentration profile using measured vacancy-mediated diffusivity and rate of exchange processes.

The most likely origin of appearance and disappearance events is exchange of embedded Cu atoms with thermal Pb adatoms and vice versa. The relative population of thermal Pb adatoms to embedded Pb atoms is given by the Boltzmann factor of their energy difference (calculated 0.38 eV). The absolute rate at which Pb adatoms embed in the surface layer is determined by this energy plus the barrier to exchange with a Cu surface atom (calculated 1.17 eV), which is 1.55 eV. This is 0.11 eV higher than the calculated energy determining the vacancy-mediated diffusion rate. At the experimental temperature of 400 K, the calculations predict a ratio between the two processes of about a factor of 25—of the same order of magnitude as measured.

Even though the exchange-reexchange process happens less frequently than vacancy-mediated diffusion, it is much more efficient at transporting and redistributing Pb atoms over long distances because of the low barrier for Pb adatom diffusion. It is therefore what mainly sets the time scale of the global approach to equilibrium. On the other hand, the local spreading of the concentration gradient depends on the rapid, short-distance, vacancy-mediated diffusion process. At higher temperatures, the long-displacement process would become even more potent because of the increase in the population of thermally generated adatoms. This idea is consistent with low energy electron microscopy measurements of the fluctuations of Pb overlayer islands on Pb/Cu(111), where kinetics appear to be dominated by a long-range adatom-mediated process at elevated temperatures [22].

In summary, diffusion of Pb in Cu(111) is not dominated by the most frequent process, or by a single less-frequent one; rather, two infrequent processes—vacancy-mediated diffusion and adatom exchange—are responsible for mass transport on different length scales. The fast processes, step-edge running and adatom evaporation and condensation at steps, do not contribute at all to the intermixing kinetics. The measured results are consistent with our first-principles total-energy calculations.

We gratefully acknowledge useful discussions with Gary Kellogg, Norm Bartelt, and Raoul van Gastel. Sandia is a multiprogram laboratory operated by Sandia Corporation, a Lockheed Martin Company, for the U.S. DOE under Contract No. DE-AC04-94AL85000. This work was supported in part by the Division of Materials Science and Engineering, Office of Science, U.S. DOE.

[1] A. K. Schmid *et al.*, Phys. Rev. Lett. **77**, 2977 (1996).
[2] R. van Gastel *et al.*, Nature (London) **408**, 665 (2000); R. van Gastel *et al.*, Phys. Rev. Lett. **86**, 1562 (2001).
[3] M. L. Grant, B. S. Swartzentruber, N. C. Bartelt, and J. B. Hannon, Phys. Rev. Lett. **86**, 4588 (2001).
[4] G. L. Kellogg, Surf. Sci. Rep. **21**, 1 (1994).
[5] P. Wynblatt and N. A. Gjostein, Surf. Sci. **12**, 109 (1968); G. De Lorenzi and G. Jacucci, Surf. Sci. **116**, 391 (1982); M. Karimi *et al.*, Phys. Rev. B **52**, 5364 (1995).
[6] M. Giesen, Prog. Surf. Sci. **68**, 1 (2001).
[7] H. C. Jeong and E. D. Williams, Surf. Sci. Rep. **34**, 175 (1999).
[8] R. Plass, J. A. Last, N. C. Bartelt, and G. L. Kellogg, Nature (London) **412**, 875 (2001).
[9] G. Kresse and J. Hafner, Phys. Rev. B **47**, 558 (1993); Phys. Rev. B **49**, 14 251 (1994); G. Kresse and J. Furthmüller, Comput. Mater. Sci. **6**, 15 (1996); Phys. Rev. B **54**, 11 169 (1996).
[10] D. Vanderbilt, Phys. Rev. B **41**, 7892 (1990); A. Pasquarello *et al.*, Phys. Rev. Lett. **69**, 1982 (1992); K. Laasonen *et al.*, Phys. Rev. B **47**, 10 142 (1993); G. Kresse and J. Hafner, J. Phys. Condens. Matter **6**, 8245 (1994).
[11] J. P. Perdew, in *Electronic Structure of Solids '91*, edited by P. Ziesche and H. Eschrig (Akademie Verlag, Berlin, 1991); J. P. Perdew and Y. Wang (unpublished).
[12] H. Jónsson, G. Mills, and K.W. Jacobsen, in *Classical and Quantum Dynamics in Condensed Phase Simulations*, edited by B. J. Berne, G. Ciccotti, and D. F. Coker (World Scientific, Singapore, 1998).
[13] C. Nagel *et al.*, Surf. Sci. **321**, 237 (1994).
[14] For the case of N atoms adsorbed on the Ru(0001) surface, the atomic-scale diffusivity is the same as that measured from the profile decay. T. Zambelli *et al.*, Phys. Rev. Lett. **76**, 795 (1996).
[15] R. van Gastel *et al.*, Surf. Sci. **521**, 26 (2002); E. Somfai *et al.*, Surf. Sci. **521**, 26 (2002).
[16] M. J. A. M. Brummelhuis and H. J. Hilhorst, J. Stat. Phys. **53**, 249 (1988).
[17] J. Bardeen and C. Herring, in *Imperfections in Nearly Perfect Crystals*, edited by W. Shockley, J. H. Hollomon, R. Maurer, and F. Seitz (Wiley, New York, 1952).
[18] M. Eisenstadt and A. G. Redfield, Phys. Rev. **132**, 635 (1963).
[19] M. Schunack *et al.*, Phys. Rev. Lett. **88**, 6102 (2002).
[20] J. Philibert, in *Atom Movements—Diffusion and Mass Transport in Solids* (Les Éditions de Physique, Les Ulis, France, 1991).
[21] D. C. Senft and G. Ehrlich, Phys. Rev. Lett. 74, 294 (1995).
[22] R. Plass, N. C. Bartelt, and G. L. Kellogg, J. Phys. Condens. Matter **14**, 4227 (2002).